

## EXPERIMENTAL INVESTIGATION OF AERODYNAMIC CHARACTERISTICS OF TWO, THREE AND FOUR BLADED S-SHAPED STATIONARY SAVONIUS ROTORS.

Md. Quamrul Islam, Md. Nasim Hasan and Sumon Saha

Department of Mechanical Engineering,  
Bangladesh University of Engineering & Technology, Dhaka-1000, Bangladesh

### ABSTRACT

In this paper, variation of static torque and drag coefficient of an S-Shaped Savonius rotor have been studied for different number of rotor blades. This has been done by measuring the pressure distribution on the blade surfaces for different rotor angles. All the experiments have been carried out at Reynolds number  $1.07 \times 10^5$  in a uniform flow jet produced by an open circuit wind tunnel. Experimental results indicate that both of the drag force and hence the torque change frequently with rotor angle. It is also found that as the increase of the number of rotor blade increases the starting torque of rotor increases but there is no significant increase in net torque output. It is observed that, torque distribution becomes more uniform as the number of blade of rotor increases.

**Keywords:** S-Shaped Savonius rotor, Static torque and drag coefficient.

### 1. INTRODUCTION

The original Savonius rotor, which was invented in 1920's in Finland. It is drag-based vertical axis wind turbine (VAWT). It can be made in many different ways with buckets, paddles, sails, and oil drums. All of these designs run relatively slowly, and has a lower efficiency compared to other vertical wind power-extracting machines. However, Savonius rotor is still popular as an alternative to extract wind power in the developing country because of its simplicity in design, ease of construction, self starting and direction independent operation at low speed [1,2,7,9]. The common use of Savonius rotor includes grinding grain, pumping water, and many other tasks. For this reason, rigorous studies have been made so far for the improvement of its aerodynamic performance. The S-Shaped rotor is a modified form of Savonius rotor with no overlap. Littler [6] first developed its optimum profile which is shown in Figure-1.

### 2. EXPERIMENTAL SET UP AND PROCEDURE

The objective of this paper work was to investigate the aerodynamic characteristics of two, three and four bladed S-Shaped Savonius rotor in a uniform flow jet, which had been done with the help of a subsonic wind tunnel, experimental set up of S-Shaped rotors with two, three and four blades and inclined manometer bank.

#### 2.1 Wind Tunnel

The schematic diagram of wind tunnel is shown in Figure-2. The open circuit subsonic wind tunnel is 6.55

m long with a test section of (490 mm x 490 mm) cross-section. The successive sections of the wind tunnel comprise of converging mouth, perspex section, rectangular section, fan section, butterfly section, silencer section, diverging section, converging section, rectangular section, flow straighter section and rectangular exit section. The rotors were placed at the jet axis and at 750 mm downstream of the exit section. The uniformity of flow was checked by determining the velocity distribution in which it was found that the velocity remains constant within the  $\pm 0.5\%$  of the centerline velocity of the test section (8.7 m/s).

#### 2.2 The S-Shaped Rotor

The S-Shaped rotor blade was made of PVC pipe and geometrically similar to that designed by Littler [6]. Three rotors were made having two, three and four blades, where the height and diameter of each rotor were 342.9 mm and 185.72 mm. The cord length of each blade is 91.44 mm. Both the top and bottom end of rotor are fitted with end caps. The pressure measurements were made at 8 pressure tappings on each blade. The tappings were located at the mid-plane of one segment of equal length on one surface of each blade as shown in Figure-3. The pressures were measured at  $20^\circ$  interval of rotor angle. The schematic diagram of two, three and four bladed S-Shaped Savonius rotor is shown in Figure-3. Different Forces acting on a blade are shown in Figure-4 for a two bladed rotor which is similar to other blades of two, three and four bladed rotors. The position of different pressure tappings for determining the forces are

shown in figure-5 for a two bladed rotor which was also done for three and four bladed rotors also.

### 3. AERODYNAMICS CHARACTERISTICS CALCULATION

The flow pattern around the rotor blade is characterized by complicated flow phenomena with high turbulence, unsteadiness and flow separation [1,9]. The combined of these flow features produces pressure differences between the front and back surfaces of the blades that result in aerodynamic forces and hence torque.

The forces acting on S-Shaped rotor can be resolved into components  $F_n$  and  $F_t$ , along normal and tangential directions of the rotor chord as shown in Figure-4. The corresponding drag coefficients can be written as:

$$C_{ni} = \frac{F_{ni}}{\frac{1}{2} \rho U_0^2 R}, \quad C_{ti} = \frac{F_{ti}}{\frac{1}{2} \rho U_0^2 R} \quad (1)$$

where subscript  $i$  indicates the pressure tapping number. The forces  $F_n$  and  $F_t$  can be evaluated from the pressure differences as:

$$F_{ni} = \Delta P_i \Delta S_i \sin \phi_i, \quad F_{ti} = \Delta P_i \Delta S_i \cos \phi_i \quad (2)$$

where  $\Delta P_i$  is the pressure difference between the front and back surfaces of the blade at a particular pressure tapping,  $i$ ;  $\phi_i$  is the angle between the normal of segment  $i$  and the direction of flow;  $\Delta S_i$  is the chord length around the tapping  $i$  where uniform pressure is assumed.  $R$  is the radius of the rotor. The normal force  $F_{ni}$  is responsible for producing a torque on the rotor shaft and this torque can be expressed for an element of the blade as:

$$T_i = F_{ni} r_i \quad (3)$$

where  $r_i$  is the distance between the center of rotor and the normal of segment  $i$ .

Torque coefficient can be found out from equation (4) as

$$C_{qi} = \frac{T_i}{\frac{1}{2} \rho U_0^2 R \frac{R}{2}} \quad (4)$$

The total drag coefficient and the torque coefficient for an individual blade at a particular rotor angle,  $\alpha$  are evaluated by integrating the coefficients over the blade surfaces.

$$C_n(\alpha) = \sum_{i=1}^8 C_{ni}, \quad C_t(\alpha) = \sum_{i=1}^8 C_{ti}, \quad C_q(\alpha) = \sum_{i=1}^8 C_{qi}$$

### 4. RESULT AND DISCUSSION

As mentioned earlier, the differences in pressure between the front and backside of the rotor blade result drag forces in normal and tangential direction. The variations of these drag coefficients are graphically presented here.

Normal drag coefficient  $C_n$  of an individual blade of two-bladed S-Shaped rotor, three-bladed S-shaped rotor

and four-bladed S-Shaped rotor is shown here in Fig. 5. In case of two bladed rotor it increases from  $\alpha=0^\circ$  rotor angle and maximum positive normal drag occurs at  $\alpha=60^\circ$  and then remains constant up to rotor angle  $140^\circ$ . There is a drastic drop in normal drag between  $\alpha=140^\circ$  and  $160^\circ$ . Between  $\alpha=160^\circ$  and  $180^\circ$  a small positive drag exists up to  $180^\circ$ . But after  $\alpha=180^\circ$  there exists a negative drag up to  $360^\circ$  with a minimum value at  $300^\circ$ . The value of  $C_n$  decreases smoothly from  $\alpha=180^\circ$  to  $260^\circ$  and then sharply drops up to  $\alpha=300^\circ$  and then increases up to  $\alpha=0^\circ$ . For the flow over three bladed-rotor maximum positive normal drag occurs at  $\alpha=40^\circ$  and then decreases smoothly as compared with 2-blade rotor up to  $\alpha=140^\circ$ . Negative drag exists in the region  $180^\circ$  to  $360^\circ$  but of greater magnitude than 2-blade rotor. The minimum value of  $C_n$  occurs at  $\alpha=300^\circ$  of rotor angle. In case of four bladed rotor  $C_n$  increases  $\alpha=0^\circ$  to  $40^\circ$  with maximum drag at  $40^\circ$  rotor angle. Then it remains constant up to  $\alpha=80^\circ$  rotor angle. The value of  $C_n$  decreases sharply between  $\alpha=80^\circ$  to  $100^\circ$ . After that  $C_n$  remains constant up to  $\alpha=140^\circ$ . Drag coefficient then decreases smoothly up to  $\alpha=240^\circ$ . A rapid fall of  $C_n$  occurs between  $\alpha=240^\circ$  and  $290^\circ$ . The minimum value of  $C_n$  occurs at  $\alpha=290^\circ$  rotor angle. The value of  $C_n$  then increases from  $\alpha=300^\circ$  to  $0^\circ$  of rotor angle.

The tangential drag coefficient  $C_t$  of an individual blade for two bladed-system, three-bladed system and four-bladed system is shown for different rotor angle in Fig. 6. For two bladed system the tangential drag coefficient,  $C_t$  decreases from  $\alpha=0^\circ$  to  $60^\circ$ . It then increases up to  $120^\circ$  after which it remains constant more or less up to  $140^\circ$  of rotor angle. It then starts to decline and reaches to its maximum negative value at  $\alpha=260^\circ$ . The tangential drag coefficient  $C_t$  then increases sharply between  $\alpha=260^\circ$  and  $360^\circ$  reaching its maximum positive value at  $\alpha=360^\circ$ . In case of three bladed system at  $\alpha=0^\circ$  the tangential drag coefficient,  $C_t$ , is positive then decreases with rotor angle up to  $80^\circ$  reaching its minimum value at  $\alpha=80^\circ$ . It then increases from  $\alpha=80^\circ$  to  $160^\circ$ . The value of tangential drag coefficient  $C_t$  remains almost constant which is nearly zero from  $\alpha=160^\circ$  to  $220^\circ$ . Then it increases from  $\alpha=220^\circ$  to  $280^\circ$ . There is a drop in the value of  $C_t$  from  $\alpha=280^\circ$  to  $300^\circ$ . Finally, the value of tangential drag coefficient,  $C_t$  increases from  $\alpha=300^\circ$  to  $360^\circ$  where it reaches maximum positive value. For the flow over four bladed system the value of tangential drag coefficient,  $C_t$  increases from  $\alpha=0^\circ$  to  $20^\circ$  with maximum positive value at  $\alpha=20^\circ$ . It then decreases from to  $\alpha=20^\circ$  to  $120^\circ$  with its minimum value at  $\alpha=120^\circ$ . The tangential drag coefficient  $C_t$  then increases with rotor angle up to  $\alpha=220^\circ$ . Within the range  $\alpha=220^\circ$  to  $320^\circ$  the value of  $C_t$  decreases with rotor angle. Finally, there is an increase in the value of  $C_t$  between  $\alpha=320^\circ$  to  $360^\circ$ .

The torque coefficient on a single blade is shown in Fig. 7 for two-bladed rotor system, three-bladed rotor system and four-bladed rotor system. As torque coefficient is a function of normal drag coefficient and distance of normal direction from the center of rotor, so the nature of torque coefficient vs. rotor angle graph for different number of blades is of same nature as the normal drag coefficient curve

From the graphs experimentally obtained, it is evident that with the increase of the number of blade there is no significant change in the value of drag coefficient,  $C_n$  and thus of torque coefficient,  $C_q$  rather the starting torque increases slightly and is obtained at smaller value of rotor angle  $\alpha$ . Moreover, the torque distribution becomes more uniform if the number of blades increases

### 5. FIGURES

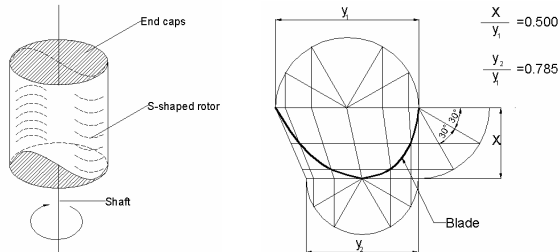
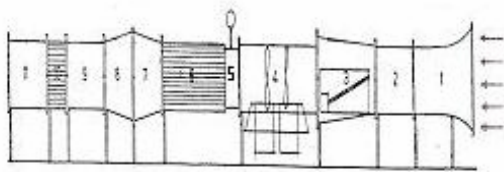


Fig 1. S-Shaped profile as developed by Littler [6]

#### 1. Converging Mouth Entry



2. Perspex Section
3. Rectangular Diverging Section
4. Fan Section
5. Butterfly Section
6. Silencer with Honeycomb
7. Diverging Section
8. Converging Section
9. Rectangular Section
10. Flow Straighter Section
11. Rectangular Exit Section

Fig 2. Schematic diagram of wind Tunnel

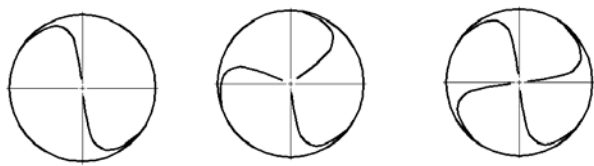


Fig 3. Two, three and four bladed S-shaped rotors

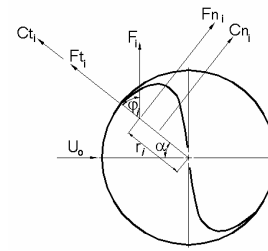


Fig 4. Forces acting on a blade of two bladed rotor.

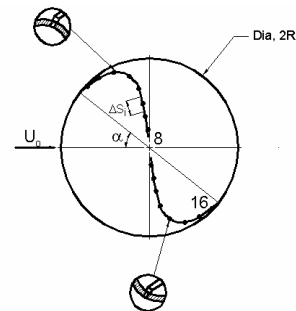


Fig 5. Positions of pressure tapings on the blades of two bladed rotor.

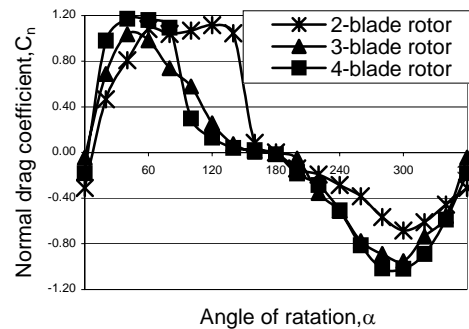


Fig 6. Variation of normal drag coefficient,  $C_n$  with rotor angle ( $\alpha$ )

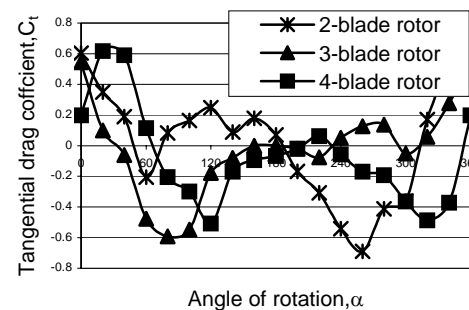


Fig 7. Variation of tangential drag coefficient,  $C_t$  with rotor angle ( $\alpha$ )

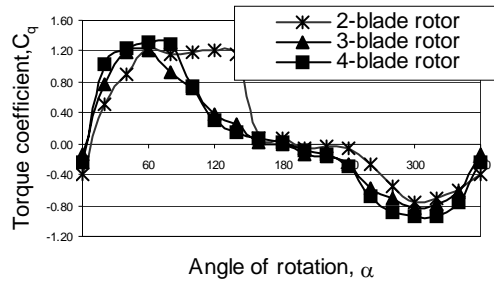


Fig 8. Variation of torque coefficient,  $C_q$  with rotor angle ( $\alpha$ )

## 6. REFERENCES

1. Aldos, T.K and Kotb, M.A. (1991), "Aerodynamic Loads on a Stationary Savonius Rotor", JSME International journal, Series II, no. 34, Japan.
2. Bhuiyan, M.H.K., "Aerodynamic Characteristics of a Four Bladed Savonius Rotor", M.Sc. Engineering Thesis (2003), Department of Mechanical Engineering, BUET, Bangladesh.
3. Fusisawa, n. (1992), "On the Torque Mechanism of Savonius rotors", Journal of Wind Engineering and Industrial Aerodynamics, No. 40, U.K.
4. Huda, M.D., Selim, M.A., Islam, A.K.M.S. and Islam, M.Q. (1992), "The Performance of an S-Shaped Savonius Rotor with a Deflecting Plate", RERIC International Energy Journal, No.14., Bangkok, Thailand.
5. Islam, A.K.M.S., M.Q., Mandal A.C and Razzaque, M.M. (1993), "Aerodynamic Characteristics of a Stationary Savonius Rotor", RERIC International Energy Journal, No.15, Bangkok, Thailand.

6. Littler, R.D (1975), "Further Theoretical and Experimental Investigation of the Savonius Rotor", B.E. Thesis , University of Queensland, Australia.
7. Lysen, E.H., Bos, H.G and Cordes, E.H. (1978), "Savonius Rotors for Water Pumping", SWD publications, P.O. Box 85, Amersfoort, The Netherlands
8. Rahman, M., "Aerodynamic Characteristics of a Three Bladed Savonius Rotor", M.Sc. Engineering Thesis(2000), Department of Mechanical Engineering, BUET.
9. Sawada T., Nakamura, and Kamada, S. (1986), "Blade Force Measurement and flow visualization of Savonius Rotors", Bull. JSME, Vol.29, Japan.

## 7. NOMENCLATURE

Symbol	Meaning	Unit
$\Delta P_i$	Pressure difference	(Pa)
$F_n$	Normal Force	(N)
$F_t$	Tangential Force	(N)
$C_n$	Normal drag coefficient	
$C_t$	Tangential drag coefficient	
$T$	Torque	(N-m)
$C_q$	Torque coefficient	
$R$	Rotor radius	(m)
$r_i$	Distance between rotor center and normal of any segment, $i$ .	(m)
$\Delta S_i$	Chord length of any segment	(m)
$\phi_i$	Normal angle	Degree